MINERALOGICAL MAGAZINE, SEPTEMBER 1981, VOL. 44, PP. 315-23

Upper-mantle metasomatism beneath a continental rift: clinopyroxenes in alkali mafic lavas and nodules from South West Uganda

F. E. LLOYD

Department of Geology, University of Reading

ABSTRACT. Clinopyroxenes are dominant in highly potassic, silica undersaturated mafic volcanics occurring on the western rim of the uplifted, rifted East African craton. A kimberlite style of eruption provides nodules of alkali clinopyroxenite (clinopyroxene + titaniferous phlogopite + titanomagnetite, apatite, sphene, and rare corroded olivine) which have similar bulk chemistry to the feldspathoid-bearing lavas. Many nodules display metasomatic textures supporting a formation from the alteration of pre-existing material; clinopyroxene growth is characterized by complex, non-oscillatory colour zoning. Comparison of natural clinopyroxene chemistry with published data for clinopyroxenes crystallized from synthetic potassium-rich mafic material, suggests that a significant proportion of the nodules crystallized at upper-mantle pressures. Neither garnet- nor ortho-pyroxene-bearing nodules have ever been recorded from south-west Uganda, suggesting that metasomatism of the local mantle has proceeded far enough to obliterate all recognizable remnants of four-phase lherzolite.

THE Quaternary to Recent volcanics of south-west Uganda are notable amongst alkaline provinces for unusual enhancement in potassium, particularly in the fields of Katwe–Kikorongo and Bunyaruguru on which this study is focused. Here potassium levels are matched only in volcanics from Murcia and Almeria in southern Spain (Borley, 1967), Leucite Hills in Wyoming USA (Carmichael, 1967), West Kimberley in Australia (Wade and Prider, 1940), and the Roman Province, Italy (Savelli, 1968). The problem of these potassic mafic lavas is that derivation from accepted mantle assemblages (spinel lherzolite, garnet peridotite, pyrolite, etc.) requires a means of concentrating potassium and residual elements that is capable of producing extreme enrichment factors (>200 for K in the Ugandan lavas).

These unusual volcanics are found in the west branch of the vast East African rift system. As in other rifted areas, there is a close relationship between rifting and spectacular doming of the continental crust (Bailey Willis, 1936; King, 1962; Holmes, 1965), and a close association with highly alkaline, volatile-rich volcanism unparalleled in other tectonic settings (Holmes, 1950, 1965; Bailey, 1964, 1972, 1974; Lloyd and Bailey, 1975).

Bailey (1972) developed the hypothesis that bending and fissuring of the continental lithosphere during drift localizes mantle degassing. Volatiles flow into arches and tensional regions of the lithosphere locally metasomatizing the mantle to a composition of alkali peridotite, causing uplift and rifting. Lloyd and Bailey (1975) showed that a mantle of this composition is consistent with low seismic velocities immediately below the rifted crust of East Africa and the Rhein valley, West Germany (Long *et al.*, 1972; Mueller *et al.*, 1969). This proposition leads to the prediction that the mantle beneath an uplifted, rifted continental region of alkaline activity like south-west Uganda, should be highly unusual. This prediction is supported by the composition of the nodules from this region.

Petrography of the nodules

In the nodules, dominant clinopyroxene (showing complex colour zoning) is found with titaniferous phlogopite, rarely amphibole, titanomagnetite, sphene, apatite, and also calcite in carbonatitic examples. Modal mineralogy and texture are very variable; in common with the other nodule minerals clinopyroxene shows a large range of grain size (4.00–0.01 mm diam.) and shape, is patchy in distribution, and often forms monomineralic bands and lenses. Broadly, two major types of clinopyroxene nodule are recognized.

(i) Closely textured nodules with anhedral interlocking grains that have few interstices. These nodules sometimes show deformation features more common to anhydrous species (lherzolite, dunite, etc.), e.g. granulation and recrystallization of grain borders, kinked micas and, rarely, fracture cleavage of clinopyroxene.

(ii) Nodules where the larger clinopyroxenes and phlogopites form a framework of interfering plates and laths. These spaces are usually filled by smaller clinopyroxenes and phlogopites plus apatite, titanomagnetite, and sphene; occasionally they form holes.

In addition there are rare nodules that do not belong to (i) or (ii), such as apatite-rich nodules composed of euhedral to subhedral clinopyroxene, apatite, and ore in a browny-green glass; carbonatitic nodules—fragmental clinopyroxene and phlogopite in a matrix of calcite, apatite, and sphene; and one amphibole-rich clinopyroxenite, S23212.

Garnet and orthopyroxene have never been recorded from the nodules of south-west Uganda. Nodules in the Bufumbira volcanics, to the south, may contain olivine, but this mineral is rare in the nodules from Katwe-Kikorongo and Bunyaruguru and occurs as isolated grains which are often corroded and enclosed by hydrous minerals.

Closely textured nodules (type i) and carbonatitic nodules, in particular, display notable alteration features which are *not marginal* but developed *within* the nodules showing that their mineralogy is the product of metasomatism of pre-existing material (Lloyd and Bailey, 1975).

Petrography of the lavas

The lavas are largely pyroclastic—ejected lava blocks, bombs, lapilli, and crystal lapilli (phlogopite and clinopyroxene) which, together with occasional ultramafic nodules, are cemented into tuffs by calcium carbonate. There are eleven small lava flows.

Pale-brown clinopyroxene is the dominant mineral in flows and ejected blocks. It forms both phenocrysts and groundmass minerals together with titanomagnetite, perovskite, and sometimes olivine. Clinopyroxene phenocrysts may display dark-green pleochroic cores. Alkali enrichment and silica undersaturation are reflected in modal proportions of late crystallizing feldspathoids (leucite, nepheline, and kalsilite) and phlogopite.

Wherever they are found, small bombs and lapilli are distinctive, being always composed of olivine and melilite set in a dark glass. Pale-green clinopyroxene forms sparse phenocrysts of xenocrystic appearance.

In addition, one ejected block of nepheline leucitite was found, S23 173. This specimen is unusually felsic and is the only lava with dark-green clinopyroxene, which occurs as phenocrysts and groundmass minerals; the phenocrysts are euhedral but broken (fig. 2*b*). This lava block also contains fragments of apatite dinopyroxenite.

Are the nodules mantle material?

At this stage this question must be asked. If so, are they derived from a mantle that has been modified by metasomatism prior to eruption, i.e. by volatile fluxing (Bailey, 1972), or do they represent mantle material (possibly spinel or garnet lherzolite) that has been modified by metasomatism during or after eruption? Some clues are provided by the petrography. The deformation features of

TABLE I. *Types of clinopyroxene zoning*

	Zone type	Nodule	Lava
a	Pleochroic patches of dark-green sahlite in non-pleochroic grains of pale sahlite. Fig. 1*a*	In type i nodules, with phlogopite, minor ore, apatite, sphene, and trace olivine	Not represented
b	Corroded green sahlite cores in neutral diopside envelopes, sometimes with oscillation banded purplish-brown borders. Fig. 1*b*	In type ii nodules, with phlogopite, minor ore, apatite, and sphene	Commonly represented in phenocrysts. Fig. 2*a*
c	Pale sahlite core zoning to darker-green sahlite envelope, in euhedral to subhedral prisms. Fig. 1*c*	In apatite-rich nodules, with titanomagnetite in glass	Sahlite phenocrysts of similar appearance, in unusual leucitite lava, S23 173. Fig. 2*b*
d	Abrupt transition from anhedral neutral diopside core to ragged augite-ferroaugite envelope. Fig. 1*d*	In carbonatitic nodules, with phlogopite-biotite, apatite, sphene, and calcite	Not represented
e	Irregular envelope of dark-green sahlite around anhedral pale sahlite core. Fig. 1*e*	In one amphibole-rich nodule, S23 212, with trace apatite and sphene	Not represented

the closely textured nodules (type i) are considered in lherzolites to be indicative of subsequent tectonic processes in the predominantly solid state at comparatively low temperatures (Den Tex, 1971). This implies they are derived from material that has existed at depth for a considerable period. Metasomatic textures in these nodules suggest derivation from altered mantle material. The only clue to the nature of the original material is given by isolated grains of olivine reacting out to form hydrous minerals. If this is all that remains of (?)lherzolite, it is unlikely that such all-pervasive metasomatism took place during or after eruption.

The large framework-forming laths of type ii nodules give the appearance of accumulation from a liquid, which continued to crystallize in the spaces between the larger crystals. Where these spaces are empty, i.e. form holes, there is no evidence (in the form of glass) that they ever contained silicate liquid. Presumably they were filled with volatiles.

What evidence have we of a high-pressure origin for the nodules? Did any of the minerals form at mantle depths? In an attempt to answer this question the clinopyroxene chemistry of nodules and lavas was investigated. Clinopyroxene is the dominant phase and shows complex zoning and alteration which ought to throw light on the origin and evolution of this enigmatic nodule suite.

Clinopyroxene chemistry

The petrography of the clinopyroxenes and their zones is summarized in Table I and figs. 1 and 2. The chemistry of the zoning was investigated by means of electron microprobe. Representative analyses (selected from 123 spot determinations) are

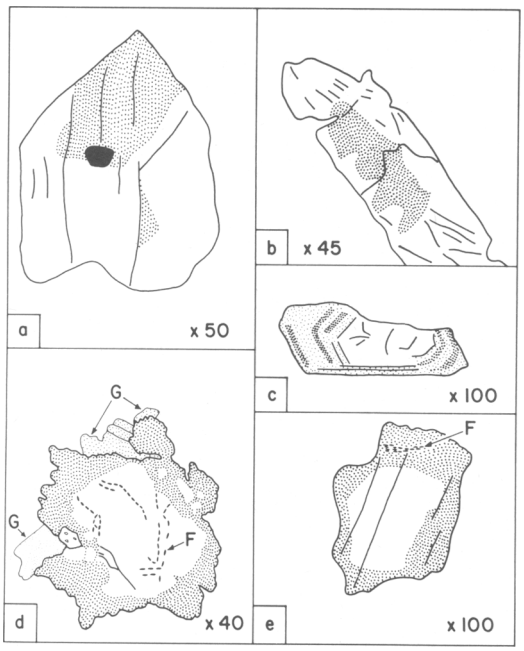

FIG. 1. Colour zoning and patterns in nodule clinopyroxenes: darker-green parts shaded (traced from photomicrographs). (*a*) Clinopyroxene grain from type i nodule S23 214 (Chabachu Crater, Bufumbira). Dark-green sahlite patches in pale-green sahlite which encloses ore grain (solid). (*b*) Clinopyroxene lath from type ii nodule S23 209 (Nabugando Crater, Katwe–Kikorongo). Anhedral green sahlite core in pale-brown diopside envelope. (*c*) Clinopyroxene lath from apatite-rich nodule S23 211 (Nabugando Crater, Katwe–Kikorongo). Paler-green sahlite core zoned via oscillation banding to darker-green sahlite envelope. (*d*). Clinopyroxene 'phenocryst' in carbonatitic nodule S23 210 (Nabugando Crater, Katwe–Kikorongo). Neutral diopside core with fluid inclusion trains (F), surrounded by ragged dark-green augite–ferroaugite envelope, which encloses some fragments of diopside core. Groundmass grains (G) are of ferro-augite composition. (*e*) Clinopyroxene grain from amphibole-rich nodule S23 212 (Crater N. of Nabugando, Katwe–Kikorongo). Anhedral pale-green sahlite core in dark-green sahlite envelope containing fluid inclusion train (F).

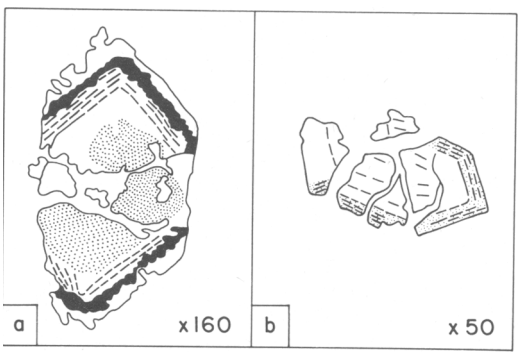

FIG. 2. Types of zoning in lava clinopyroxenes (traced from photomicrographs). (*a*) Clinopyroxene phenocryst from alkali clinopyroxenite lava S23 160 (Nabugando Crater, Katwe–Kikorongo). Anhedral green sahlite core, partially surrounded by neutral diopside zone darkening to zone of purplish-brown oscillation banded diopside; followed outwards by band of corrosion (solid) with outer edging of ragged neutral diopside. The deep central embayments are now filled by groundmass. NB. No chemical difference between neutral and brown diopside was discernible, except a tendency for the brown variety to be enhanced in Ti, therefore they have been grouped together as envelope clinopyroxene on chemical variation diagrams. (*b*) Clinopyroxene phenocryst from nepheline leucitite lava S23 173 (Mahega Crater, Katwe–Kikorongo). Green sahlite zoning from paler core to darker envelope via oscillation bands. Euhedral outline is broken up by a pattern of cracks filled with groundmass.

given in Table II. All analysed clinopyroxenes were found to be Ca-rich, with the majority plotting slightly in excess of Ca45 atomic per cent, at the base of the diopside and sahlite fields on the pyroxene quadrilateral of Poldervaart and Hess (1951). A few analyses fall into the upper portion of the augite and ferroaugite fields. Al contents are notably low, with the majority of values falling between 0.05 and 0.175 ions on the basis of 6 oxygens. Ti is also low and varies from 0.10 ions per unit formula in sahlite from apatite-rich nodule S23 211, to below detection in ferroaugite rims of carbonatitic clinopyroxene S23 210 (Table II). Clinopyroxenes from other highly potassic volcanics of Murcia, Spain; Leucite Hills, Wyoming, USA; and West Kimberley, Western Australia, are similarly high in Ca and low in Al and Ti (Carmichael, 1967).

The chemical variations shown by the zoned clinopyroxenes can be discussed with reference to Table II and fig. 3. The trend in fig. 3 largely reflects diminishing Mg^{2+} at the expense of increasing

TABLE II

REPRESENTATIVE ELECTRON MICROPROBE ANALYSES OF UGANDAN CLINOPYROXENES

	S23, 214		S23, 209		S23, 160		S23, 165	S23, 211		S23, 173	
	86	101	30	28	48	46	36	79	80	24	22
SiO_2	52.30	52.53	51.78	50.06	52.89	50.68	49.59	47.93	45.35	49.61	46.01
TiO_2	1.03	0.81	1.83	1.53	1.00	0.44	3.33	1.84	2.36	0.91	1.46
Al_2O_3	2.25	2.15	2.24	3.47	0.58	1.32	3.82	4.21	5.14	2.48	5.59
Fe_2O_3**				4.01	3.01	8.14	2.09	7.45	10.99	8.19	10.20
FeO	6.56	11.19	4.49	6.09	1.60	4.94	4.18	4.24	2.04	5.68	4.36
MnO	0.03	N.D.	0.20	0.34	0.11	0.45	0.27	0.02	0.05	0.47	0.47
MgO	13.59	10.95	15.81	11.59	15.65	10.26	13.72	12.02	11.91	9.43	8.42
CaO	23.52	21.81	24.39	23.44	24.86	22.25	24.02	23.49	22.93	22.74	21.45
Na_2O	0.80	1.32	0.39	0.86	0.54	1.88	0.53	0.66	0.58	0.96	1.93
TOTAL	100.08	100.76	101.20	101.39	100.24	100.36	101.36	101.86	101.35	100.47	99.89
Si	1.94	1.96	1.94	1.86	1.94	1.91	1.82	1.78	1.70	1.89	1.76
Al	0.10	0.10	0.06	0.15	0.02	0.06	0.16	0.18	0.23	0.11	0.25
Fe^{3+}				0.11	0.08	0.23	0.06	0.21	0.31	0.23	0.29
Ti	0.03	0.02	0.03	0.04	0.03	0.01	0.09	0.05	0.07	0.03	0.04
Fe^{2+}	0.20	0.37	0.14	0.19	0.05	0.15	0.13	0.13	0.06	0.18	0.14
Mn			0.01	0.01		0.01	0.01			0.01	0.01
Mg	0.75	0.59	0.87	0.64	0.86	0.58	0.75	0.67	0.63	0.54	0.48
Ca	0.93	0.88	0.92	0.93	0.98	0.90	0.94	0.93	0.93	0.93	0.88
Na	0.06	0.07	0.02	0.06	0.04	0.14	0.04	0.05	0.07	0.07	0.14
CATION SUM*	4.01	3.99	3.99	3.99	4.00	3.99	4.00	4.00	4.00	3.99	3.99

Analyst F. E. Lloyd.
*On the basis of 6 oxygens.
**Fe_2O_3 has been calculated on the basis that cation sum = 4, according to a method of A. Ferguson (Pers. Comm.).
N.D. = Not Detected.
N.A. = Not Analysed.

86 = pale salite, 101 = green patch, 30 = brown envelope, 28 = green core, 48 = neutral edge, 46 = green core, 36 = groundmass lath, 79 = pale core, 80 = darker green envelope, 24 = pale core, 22 = darker envelope, 127 = colourless core, 129 = dark green envelope, 122 = pale green core, 119 = dark green envelope, 77 = xenocryst.

	S23, 173		S23, 212		S23, 149
	127	129	122	119	77
SiO_2	51.63	52.12	50.87	46.84	48.38
TiO_2	0.77	0.22	0.38	1.59	1.17
Al_2O_3	1.85	0.74	3.57	7.55	3.34
Fe_2O_3	4.82	12.35	5.24	7.59	6.96
FeO	0.17	3.09	5.63	5.96	6.27
MnO	0.27	0.53	0.25	0.28	0.12
MgO	15.48	9.41	11.02	8.01	10.14
CaO	23.67	18.99	21.35	20.15	22.50
Na_2O	0.84	3.82	1.77	2.38	1.21
TOTAL	99.50	101.27	100.08	100.35	100.09
Si	1.90	1.94	1.90	1.77	1.84
Al	0.08	0.03	0.16	0.33	0.15
Fe^{3+}	0.13	0.34	0.15	0.21	0.20
Ti	0.02	0.01	0.01	0.04	0.03
Fe^{2+}	0.01	0.10	0.17	0.19	0.20
Mn	0.01	0.02	0.01	0.01	
Mg	0.86	0.53	0.62	0.45	0.58
Ca	0.93	0.76	0.85	0.81	0.91
Na	0.06	0.27	0.13	0.17	0.09
CATION SUM	4.00	4.00	4.00	3.98	4.00

Fe^{2+}, but sometimes the Fe increase is largely in terms of Fe^{3+}. High ferric iron is typical of the dark-green sahlites, augites, and ferroaugites (Table II) and is found in dark-green clinopyroxenes from other alkaline volcanics, e.g. from nodules of the West Eifel province (Aoki and Kushiro, 1968). In addition there is a general decrease in Ca (often with Ti) as Fe, Na, and Al increase. Details of the zoning are given below.

Zoned sahlites from S23 214, a closely textured nodule (fig. 1*a*; Table I, a). These sahlites all plot in the middle region of fig. 3, but the dark-green patches plot well to the left of the light-green clinopyroxene, being enriched in iron (Fe^{2+}) and depleted in Mg. Dark-green sahlite also shows a small increase in Na and a slight decrease in Al and Ti compared with the light-green variety (Table II, analyses 86 and 101).

Zoned clinopyroxenes from S23 209, a framework nodule (fig. 1*b*; Table I, b). The envelopes of the zoned framework-forming clinopyroxenes are diopside and plot to the right in fig. 3. They enclose green sahlite cores much decreased in Mg but enhanced in iron (Fe^{3+}) and which plot in the middle region of fig. 3. The cores are marginally enhanced in Na and Al and slightly depleted in Ca and Ti compared with the envelopes (Table II, analyses 30 and 28).

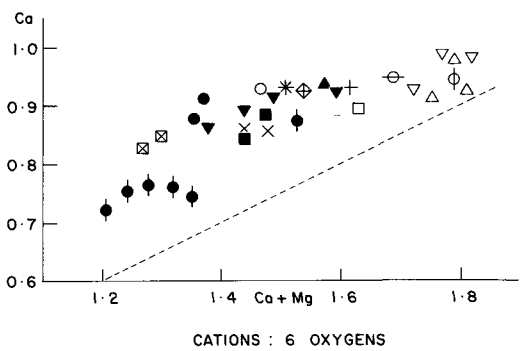

FIG. 3. Ugandan clinopyroxene compositions in terms of Ca *v.* Ca + Mg (numbers of ions on the basis of six oxygens). Dashed line represents Ca/(Ca + Mg) = 0·5. Symbols for clinopyroxenes from the different nodules and lavas are as follows: Type i nodule S23 214; pale sahlite = open squares, green patches = closed squares. Type ii nodule S23 209; pale-brown envelopes = open triangles, green cores = closed triangles. Clinopyroxenite lava S23 160; (phenocryst) pale-brown and neutral envelopes = open inverted triangles, phenocryst green cores = closed inverted triangles. Apatite-rich nodule S23 211; pale kernels = +, darker mantles = + within diamond. Leucitite lava S23 173; phenocryst pale-green cores = open circles, phenocryst darker-green envelopes = closed circles. Carbonatitic nodule S23 210; neutral cores = open circles with vertical bar, dark-green overgrowths = closed circle with vertical bar. Amphibole-rich nodule S23 212; pale cores = X, dark green envelopes = X inside square. Lapillus S23 149; pale-green xenocryst = *. Lavas S23 160 and S23 165; groundmass laths = open circle with horizontal bar. Where points cluster too closely, for clarity an average position has been plotted.

Oscillation-banded sahlite from apatite-rich nodule S23 211 (fig. 1*c*; Table I, c). Both cores and rims plot in the middle region of fig. 3 and the composition gap between cores and rims is less marked than in other examples. The darker rims plot to the left of the cores, showing a slight decrease in Mg together with an increase in Al and Ti, but the greatest change is in the state of Fe, which is considerably more oxidized in the rims (Table II, analyses 79 and 80).

Zoned 'phenocrysts' from carbonatitic nodule S23 210 (fig. 1*d*; Table I, d). The cores are diopside and plot to the right in fig. 3 with diopside from the framework nodule, but the envelopes are ferroaugite and plot to the far left, showing a remarkable fall in Mg and Ca levels together with a marked increase in Fe (Fe^{2+} and Fe^{3+}) and Na. Secondary groundmass clinopyroxene has the same composition as the 'phenocryst' envelopes. Clinopyroxenes from this nodule are particularly low in Al and Ti, both of which attain their lowest values in the rims (Table II, analyses 127 and 129).

Zoned sahlites from amphibole-rich nodule S23 212 (fig. 1*e*; Table I, e). Pale sahlite cores plot to the right of the middle region of fig. 3, together with the sahlites from the closely textured nodule, but the dark-green rims plot to the far left and are considerably enhanced in Al and Fe (Fe^{2+} and Fe^{3+}), and to a lesser degree in Na and Ti, while being depleted in Si, Mg, and Ca (Table II, analyses 122 and 119).

Zoned clinopyroxene phenocrysts from S23 160, an ejected lava block (fig. 2*a*; Table I, b). These resemble clinopyroxenes in the framework nodule, being composed of diopside rims that plot to the right in fig. 3 and green sahlite cores that plot in the middle region. Compared with the rims, the cores are depleted in Mg and to a lesser extent in Ca and Ti, but enhanced in Fe (Fe^{2+} and Fe^{3+}) and to a smaller degree in Na and Al (Table II, analyses 48 and 46).

Sahlite phenocrysts from ejected block of leucitite lava, S23 173 (fig. 2*b*; Table I, c). In appearance these resemble the clinopyroxenes from apatite-rich nodules, but they differ in chemistry, both cores and envelopes being less magnesian. The envelopes plot to the extreme left of the middle region of fig. 4, and to the left of the cores, being decreased in Mg, Ca, and Si and, to a lesser extent Fe^{2+}, but enriched in Fe^{3+}, Na, Al, and Ti.

Groundmass laths from lavas S23 160 (ejected block) and S23 165 (flow) and a pale green (?)xenocryst from a lapillus (S23 149) were also analysed. The groundmass laths plot to the right in fig. 3 with slightly lower Mg and Ca than the diopside envelopes of phenocrysts from S23 160. They also show a tendency to be less oxidized (Table II, analysis 36). The (?)xenocryst is sahlite and plots in the middle region of fig. 3.

Experimental information

Edgar *et al.* (1976) crystallized clinopyroxenes from synthetic phlogopite-rich mafurite (a type lava from Bunyaruguru), which is highly potassic and

of olivine, phlogopite, kalsilite clinopyroxene mineralogy. Crystallization took place in runs of 10–30 kbar, between 1050 and 1250 °C with varying water contents. The synthetic clinopyroxenes were found to resemble the natural types in being Ca-rich and poor in Al and Ti, a paucity striking when compared with clinopyroxenes crystallized experimentally from basanites and nephelinitic magmas (Bultitude and Green, 1971; Green, 1973*a*), and also when compared with naturally occurring clinopyroxenes from the more sodic rift valley province of the West Eifel (Aoki and Kushiro, 1968). Edgar *et al.* (1976) suggest that a high concentration of K atoms may inhibit formation of Ca–Al and Ca–Ti bonds and of $MgSiO_3$-silicate chains within the melt. If bulk chemistry of the melts affects the chemistry of the crystallizing clinopyroxene (at a range of pressures and temperatures), then clinopyroxenes cannot be used as simple geothermometers or geobarometers.

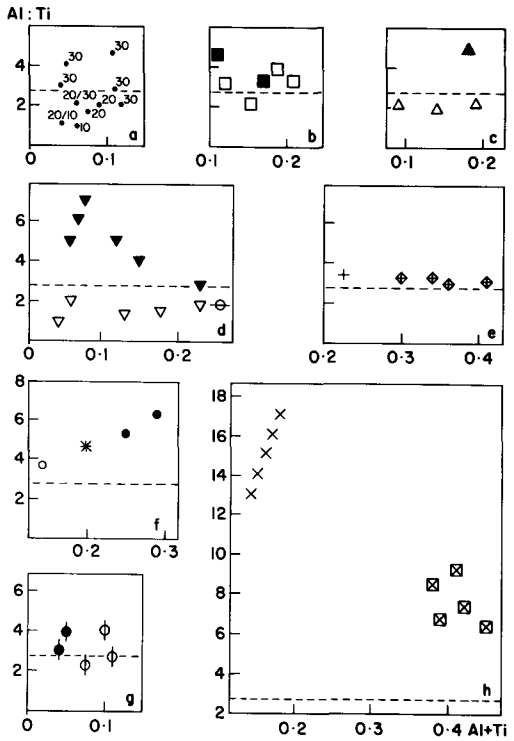

FIG. 4. Ugandan clinopyroxene compositions, natural and synthetic, in terms of Al:Ti *v.* Al+Ti (numbers of ions on the basis of 6 oxygens). All abscissae = Al+Ti, ordinates = Al:Ti. Dashed line Al:Ti = 2·6 marks boundary between region of lower pressure runs (10 and 20 kbar) and higher pressure runs (30 kbar). Symbols as for fig. 3. Clinopyroxenes from the different nodules and lavas have been plotted separately for clarity. Where points cluster too closely an average position has been taken. (*a*) Experimental clinopyroxenes of Edgar *et al.* (1976). 10 = 10 kbar, 20 = 20 kbar, 30 = 30 kbar. (*b*) Clinopyroxene analyses for type i nodule S23 214. (*c*) Clinopyroxene analyses for type ii nodule S23 209. (*d*) Clinopyroxene analyses for alkali clinopyroxenite lava S23 160 (symbol for groundmass lath represents analyses from lava S23 160 and alkali clinopyroxenite lava S23 165). (*e*) Clinopyroxene analyses for apatite-rich nodule S23 211. (*f*) Clinopyroxene analyses for nepheline leucitite lava S23 173 and lapillus S23 149 (xenocryst enclosed by lapillus). (*g*) Clinopyroxene analyses for carbonatitic nodule S23 210. (*h*) Clinopyroxene from amphibole-rich nodule S23 212. NB. The marked alignment of core analyses and marked composition gap between core and envelope (this presumably represents a decrease in pressure). The clinopyroxenes from this nodule have considerably greater Al:Ti values than those from the other investigated nodules.

It has been suggested that the relative proportion of Al in the tetrahedral site to that in the octohedral site of clinopyroxenes may be related to pressure and temperature, pressure favouring the octohedral sites (Thompson, 1947; Aoki and Kushiro, 1968). Interpreting pressures of crystallization for Ugandan clinopyroxenes using this criterion is open to the problem of melt chemistry, mentioned above, and in addition, nearly all investigated Ugandan clinopyroxenes coexist with another aluminous phase, usually phlogopite. The synthetic clinopyroxenes crystallized by Edgar *et al.*, from a K-rich melt and coexisting with phlogopite, show some tendency for Al^{vi} to increase with pressure. Out of six runs at 30 kbar, four had clinopyroxenes with $Al^{vi}:Al^{iv}$ values that accord with those from inclusions in basaltic rocks (Aoki and Kushiro, 1968), but clinopyroxenes from two 30-kbar runs, four 20-kbar runs, and three 10-kbar runs have no Al in the octohedral site.

Edgar *et al.* found that consideration of Al together with Ti suggested a pressure relationship. The Ti content of their synthetic Ugandan clinopyroxenes showed a systematic inverse relation to pressure, and plotting of Ti *v.* Al substitution indicated a further pressure dependence: Ti+2Al [for ?(Mg+2Si)] at 30 kbar, but Ti+Al [for ?(Mg+Si)] at 10 kbar. In an attempt to establish the depth at which the natural Ugandan clinopyroxenes formed, they are compared with the synthetic products on an Al:Ti *v.* Al+Ti plot, fig. 4. On this plot the experimental clinopyroxenes show increasing Al:Ti with pressure (fig. 4*a*). Variations in plot positions of clinopyroxenes crystallized at the same pressure in different runs probably arises from variations in temperature, percentage added water, and coexisting phases (NB all coexist with phlogopite). Many of the synthetic compositions plot on top of the natural compositions. Two out of the six 30-kbar runs crystallized clinopyroxenes that plot with the products of

20-kbar runs (below Al:Ti = 2.6); the two runs cannot be singled out in terms of T, P_{H_2O}, or phases coexisting with clinopyroxene. The value Al:Ti = 2.6 is used as a reference line on fig. 4 to aid discussion. It separates the clinopyroxenes from the highest pressure (30 kbar) runs from those of the lower pressure runs. The zoned clinopyroxenes plot as follows:

Zoned sahlites from S23 214, a closely textured nodule (fig. 4*b*). The majority of pale-green sahlite analyses and all analyses from the dark-green patches plot above Al:Ti = 2.6.

Zoned clinopyroxenes from S23 209, a framework nodule (fig. 4*c*). Diopside envelopes plot below Al:Ti = 2.6, but the sahlite cores plot above with clinopyroxenes from 30-kbar runs.

Oscillation banded sahlite from apatite-rich nodule S23 211 (fig. 4*e*). All analyses of these sahlites plot just above Al:Ti = 2.6; Al+Ti increases from cores to envelopes, but the Al:Ti values do not change.

Zoned 'phenocrysts' from carbonatitic nodule S23 210 (fig. 4*g*). Approximately 50% of diopside core analyses plot above Al:Ti = 2.6, together with all plottable analyses of the ferroaugite envelopes (in some, Ti falls below detection level).

Zoned sahlites from amphibole-rich nodule S23 212 (fig. 4*h*). Both kernels and envelopes of these sahlites plot with notably high Al:Ti values, higher than any other analysed Ugandan clinopyroxenes, and higher than any from the experimental runs. The ratio in the pale-green kernels is significantly higher than in the dark-green envelopes.

Zoned clinopyroxene phenocrysts from S23 160, an ejected lava block (fig. 4*d*). These phenocrysts show a similar pattern to zoned clinopyroxenes from a framework nodule; diopside envelopes plot below Al:Ti = 2.6, and sahlite cores plot above with clinopyroxenes from 30-kbar runs.

Sahlite phenocrysts from ejected block of leucitite lava, S23 173 (fig. 4*f*). These lava phenocrysts plot above Al:Ti = 2.6 and there is a marked increase in Al:Ti values from cores to envelopes.

Groundmass laths from lavas S23 160 and S23 165 both have Al:Ti values that accord with those of clinopyroxenes crystallized from 10- and 20-kbar runs (fig. 4*d*). A sahlite (?)xenocryst from a lapillus (S23 149) plots with clinopyroxenes crystallized from 30-kbar runs, above Al:Ti = 2.6 (fig. 4*f*).

Considerations

The experimental temperatures at which the clinopyroxenes were crystallized range from 1050 to 1250 °C. These are high when set against the local sub-cratonic geotherm of 30 °C per kbar, where 950 °C would be a realistic temperature at a depth relating to 30 kbar (90 km). Green (1973*b*) showed that at 30 kbar the region for incipient melting of pyrolite is 1000–1150 °C. Kushiro (1970) showed that a diopside–phlogopite assemblage is stable up to 32 kbar at 1000 °C. Thus 950 °C is too low for melts, and metasomatic textures in closely textured and carbonatitic nodules confirm this. Thus a note of caution must be introduced, when comparing synthetic clinopyroxenes crystallized from melts with natural species formed metasomatically at lower temperatures. Influx of volatiles, transferring heat and metasomatizing the mantle (Bailey, 1972), can raise the local geotherm and allow some incipient melting, but more pervasive melting will result in volcanism. These comments apply particularly to the amphibole-bearing nodule. If amphibole is to be considered stable at 30 kbar, temperatures would have to be below 800 °C (Kushiro, 1970). Fig. 4 implies that the clinopyroxene coexisting with amphibole has formed at a higher pressure than the clinopyroxenes coexisting with phlogopite, but this is unlikely when amphibole has a lower stability than phlogopite, and is at its limit at 30 kbar. This amphibole-bearing nodule is an anomaly in the Ugandan fields and has sodic bulk chemistry. Evidence suggests that clinopyroxenes from sodic melts are more aluminous than those from potassic melts, and it is inappropriate to apply the PT constraints of the Al:Ti *v.* Al+Ti plot to the clinopyroxene from this nodule.

A further consideration is that on the Al:Ti *v.* Al+Ti plot no natural Ugandan clinopyroxenes plot below synthetic varieties crystallized at 10 kbar (~ base of crust). This obviously cannot apply to most lava clinopyroxenes, especially groundmass laths which coexist with feldspathoids. No feldspathoids were encountered in 10-kbar runs between 1050 and 1500 °C (Edgar *et al.*, 1976), and it is probably incorrect to compare the lava clinopyroxenes with the experimental varieties because they do not coexist with the same Al- and Ti-bearing phases. In both nodules and experimental charges phlogopite is the coexisting Al- and Ti-(with Ti ores) bearing phase. In the lavas the major Al-bearing minerals are feldspathoids; phlogopite is a minor or trace xenocryst and groundmass mineral. These comments also apply to the apatite-rich nodule which lacks phlogopite; in this nodule glass is the other major aluminous phase.

It should also be recognized that the synthetic clinopyroxenes of Edgar *et al.*, have a more restricted range of composition than the natural Ugandan clinopyroxenes. In particular, many of the natural compositions are more Na- and Fe-rich as well as having higher levels of Al and Ti (fig. 4). This may be the consequence of a restricted starting composition for the experiments, i.e. biotite mafurite, extreme in K enrichment (even in the Ugandan fields) and with less than 1% soda. The range of chemistry for both nodules and lavas in

Katwe-Kikorongo and Bunyaruguru is considerable; though all compositions are enhanced in K, some are moderately enriched in Na as well (Lloyd, 1972).

Conclusions

The complete absence of orthopyroxene- and garnet-bearing nodules is not likely to result from lack of mantle sampling—the kimberlitic style of eruption together with the Mg, Cr, and Ni contents of the products suggests a mantle derivation for the volcanics and a mantle *origin* for some of the nodules. Absence of nodules of typical mineralogy means *atypical* mantle beneath the West Rift, of dominantly phlogopite clinopyroxenite mineralogy. Lloyd and Bailey (1975) showed a metasomatic transition between spinel lherzolite and alkali clinopyroxenite from the rift valley volcanics of the West Eifel, giving an example where typical mantle has been altered to an atypical hydrous mineral bearing assemblage.

The mantle origin for phlogopite clinopyroxenite is supported by the fact that the high-pressure runs (10–30 kbar) of Edgar *et al.* of a Ugandan composition resulted in Ugandan nodule-type mineralogy—essentially phlogopite + clinopyroxene. The experimental work showed a disappearance of olivine at the lower temperatures with increasing pressure. Olivine is rare in the nodules; when present it is corroded and altering to hydrous phases. It has been pointed out that temperatures in the subcratonic mantle would be below those of the experimental runs, and olivine recorded from the nodules may be the last remnant of four-phase lherzolite.

The closely textured nodules and the rare carbonatitic nodules are probably of mantle origin. Most analyses of their clinopyroxenes plot in the high-pressure region of fig. 4, the few that plot below this may be the result of overprinting of low-pressure effects as the nodules were brought to the surface. Deformation features occasionally found in the closely textured nodules are consistent with long residence in the solid state at depth. The subhedral laths of the framework nodules, however, give the appearance of accumulation from a liquid. In these nodules the sahlite cores alone plot with the high-pressure clinopyroxenes; all envelope analyses plot in the low-pressure region. The cores may be remnants of mantle sahlite on which lower-pressure diopside has crystallized. It is interesting that the sahlite cores in lava phenocrysts also plot with the high-pressure clinopyroxenes in fig. 4, and it is possible that phenocrysts containing these cores represent lower-pressure diopside that has crystallized around xenocryst sahlite of mantle origin. The apatite-rich assemblage has obviously crystallized from a liquid, the residue of which is represented by glass, but the clinopyroxenes do not coexist with phlogopite making it difficult to assess a likely pressure of crystallization.

The leucitite lava, S23 173, presents a problem. It is the only lava with sahlite phenocrysts. These are euhedral but broken and have presumably suffered brittle fracture under mechanical stress. Apatite clinopyroxenite xenoliths are found in this lava, but the lava sahlites are not of the same composition as sahlites from an apatite-rich nodule. The outer zones have higher Al : Ti values than the cores and suggest an increasing pressure of crystallization. This is the only case where the data implies an increase of pressure from core to envelope, and the only mechanism that can be imagined is a change in volatile pressure (P_{H_2O} and P_{CO_2}).

Acknowledgements. My thanks are due to many colleagues in the Department of Geology, University of Reading, for much technical assistance and valuable discussion. In particular to Professor D. K. Bailey and Mr J. E. Thomas. Also to Dr J. B. Wright of the Open University for reading the manuscript and making valuable suggestions. The electron-microprobe analyses were made through the kind co-operation of the British Museum (Natural History) and the Universities of Cambridge and Durham.

REFERENCES

Aoki, K. and Kushiro, I. (1968). *Contrib. Mineral. Petrol.* **18**, 326.
Bailey, D. K. (1964). *J. Geophys. Res.* **69**, 1103.
—— (1972). *J. Earth Sci.* (Leeds), **8**, 225.
—— (1974). *The Alkaline Rocks* (J. Wiley & Sons, New York), 53.
Bailey Willis (1936). *Carnegie Inst. of Washington Publication.*
Borley, G. D. (1967). *Mineral. Mag.* **36**, 364.
Bultitude, R. J. and Green, D. H. (1971). *J. Petrol.* **12**, 121.
Carmichael, I. S. E. (1967). *Contrib. Mineral. Petrol.* **15**, 24.
Den Tex, E. (1971). *Fortschr. Mineral.* **48**, 69.
Edgar, A. D., Green, D. H., and Hibberson, W. O. (1976). *J. Petrol.* **17**, 339.
Green, D. H. (1973*a*). *Earth Planet. Sci. Lett.* **17**, 456.
—— (1973*b*). *Tectonophysics*, **17**, 285.
Holmes, A. (1950). *Am. Mineral.* **35**, 772.
—— (1965). *Principles of Physical Geology* (Thomas Nelson Ltd., London and Edinburgh, new and fully revised edn.).
Hough, F. E. (1972). Ph.D. thesis, Reading.
King, L. C. (1962). *The Morphology of the Earth* (Oliver & Boyd, Edinburgh).
Kushiro, I. (1970). *Carnegie Inst. Washington Yearb.* **68**, 245.
Lloyd, F. E. (1972). See Hough (1972).
—— and Bailey, D. K. (1975). *Phys. and Chem. of the Earth* **9**, 389.

Long, R. E., Backhouse, R. W., Maguire, P. K. H., and Sundaralingham, K. (1972). *Tectonophysics*, **15**, Special Issue—East African Rifts, 165.
Mueller, St., Petersmitt, E., Fuchs, K., and Ansorge, J. (1969). *Tectonophysics*, **8**, 529.
Poldervaart, A. and Hess, H. H. (1951). *J. Geol.* **59**, 472.
Savelli, C. (1968). *Contrib. Mineral. Petrol.* **16**, 328.
Thompson, J. B. (1947). *Bull. Geol. Soc. Am.* **58**, 1232.
Wade, A. and Prider, R. T. (1940). *Q.J. Geol. Soc. Lond.* **96**, 39.

[*Manuscript received 4 August 1980; revised 24 November 1980*]